

Schrödinger cat state preparation by non-Gaussian continuous variable gate

Ivan V. Sokolov*

Saint Petersburg State University, 7/9 Universitetskaya nab., 199034 Saint Petersburg, Russia

We propose a non-Gaussian continuous variable (CV) gate which is able to conditionally produce superposition of two “copies” of an arbitrary input state well separated in the coordinate and momentum plane – a Schrödinger cat state. The gate uses cubic phase state of an ancillary oscillator as a non-Gaussian resource, an entangling Gaussian gate, and homodyne measurement which provides nonunique information about the target system canonical variables, which is a key feature of the scheme. We show that this nonuniqueness manifests problems which may arise by extension of the Heisenberg picture onto the measurement-induced evolution of CV non-Gaussian networks, if this is done in an approach commonly used for CV Gaussian schemes of quantum information.

Continuous variable quantum networks are a promising area of quantum information (quantum communication, quantum computing and simulation) [1, 2]. Since the pioneering demonstrations of CV quantum teleportation [3] and quantum dense coding [4], there was achieved an impressive progress in the theory and implementation of multimode CV cluster schemes [5–7]. Such schemes are based on Gaussian operations: the linear and bilinear in canonical variables interactions, homodyne measurements and feedforward. The large-scale CV cluster states multiplexed in the time or wavelength domain were realized and characterized [8, 9].

The CV Gaussian quantum evolution can be effectively simulated using classical computer. In order to achieve quantum supremacy, additional non-Gaussian operations are needed [1, 10]. This can be done in different approaches, including hybrid discrete- and continuous variable schemes [11, 12] or by making use of non-Gaussian Hamiltonians of the order higher than two. A cubic phase gate [13, 14] based on cubic non-demolition single-mode interaction and homodyne measurement, or higher order phase gates can serve as building blocks for universal quantum computing. Any given exponential operator of bosonic field operators, describing an arbitrary multimode Hamiltonian evolution, can be systematically decomposed into a set of universal unitary gates [15].

An implementation of cubic (or higher order) phase state meets difficulties due to weak non-linear coupling of the interacting bosons in most systems. To get around this problem, it was initially proposed [13] to prepare two quadrature entangled oscillators and to perform the ancillary oscillator homodyne measurement retaining non-linear terms which are usually omitted (see also [16]). An approximative weak cubic state described as a superposition of first low-photon Fock states was proposed [17] and experimentally prepared [18]. An approach to generating the cubic phase gate was introduced [19] where a target oscillator is repeatedly entangled with a weak coherent ancilla, and the ancilla photon subtraction or projection measurement is performed.

The general properties of the CV schemes with embedded non-Gaussian elements are actively explored today. An adaptive non-Gaussian measurement can be used in order to implement the cubic phase gate [20], and an approach was demonstrated [21] that allows effectively merge a sequence of single-mode non-Gaussian gates in order to achieve a given operation. The CV hypergraph cluster states with three-mode cubic nonlinearity can be used for universal quantum computing [22].

In this work we present a CV non-Gaussian gate which conditionally generates a Schrödinger cat state from an arbitrary target state that occupies a finite area on the phase plane. The gate exploits the same elements as the cubic phase gate introduced in [13, 14], that is, the cubic phase state, a two-mode entangling Gaussian operation, and homodyne measurement of an ancillary oscillator. As an output, a superposition of two copies of the target states well separated along the momentum axis (or, in general, along an arbitrary direction) emerge. By sequentially applying operations of this kind together with standard Gaussian gates that generate shift, rotation, squeezing, shearing, etc., one can transform an initial CV network quantum state to a Schrödinger cat state of an arbitrary complexity.

The Schrödinger cat states are an object of a relentless interest since their first introduction [23]. Besides their fundamental importance, some proposals for fault-tolerant quantum information processing directly rely on the cat-like states [13, 24].

In general, one can prepare CV Schrödinger cat states by making use of the unitary evolution assisted by a non-linear interaction, as for example in the earlier proposal [25], where a huge Kerr nonlinearity is involved. The schemes based on a measurement-induced evolution also can create cat-like states. The optical squeezed Schrödinger cat states were generated in low-photon regime using homodyne detection and photon number states as resources [26]. An iterative scheme where the target state is subsequently mixed on a passive beam-splitter with a heralded single-photon ancillary state and homodyne measurement is performed, was discussed and implemented experimentally [27, 28]. The proposals [26–28] are specifically aimed at the creation of superpositions of two coherent states.

*Electronic address: i.sokolov@mail.spbu.ru

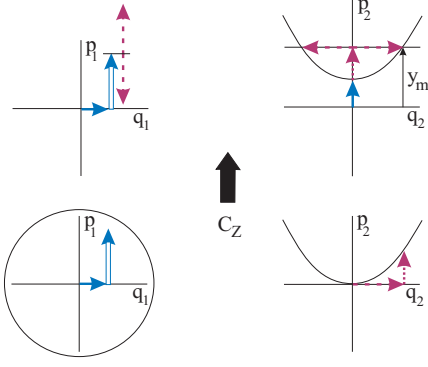


FIG. 1: Measurement-induced evolution of the position q_i and momentum p_i of the target field (left) and the ancillary oscillator (right), where the ancilla is initially prepared in cubic phase state. Here different arrows schematically represent quadrature amplitudes $\{q_i, p_i\}$ randomly chosen within the uncertainty region of the corresponding field. The ancilla wave function support is approximated with parabola, see comments in the text. The Gaussian C_Z operation entangles two oscillators. A Schrödinger cat state emerge when the ancilla momentum measurement outcome $p_2 \rightarrow y_m$ is compatible not with one, but with two clearly distinguishable values of the ancilla coordinate and, due to the entanglement, of the output field momentum. In quantum description this measurement-induced nonuniqueness may result in the output field superposition state whose components are mutually separated on the phase plane.

Unlike the previously introduced CV schemes with non-Gaussian gates, we consider measurement of the ancillary oscillator that provides nonunique information about the relevant physical variables of the target subsystem, which is a key point. This feature does not emerge in Gaussian quantum networks and manifests a superior complexity of the non-Gaussian schemes. The approach used in our proposal is scalable, that is, it can be extended to more complex CV non-Gaussian gates. From an heuristic point of view, one can easily identify some configurations where the CV cat states may arise using illustrative schemes similar to the one presented below.

The target and ancillary oscillators evolution is schematically shown in Fig. 1 which in graph form illustrates transformations of the relevant canonical variables. The ancilla is assumed to be initially prepared in the cubic phase state [13, 14] via the action of unitary evolution operator $\exp(i\gamma q_2^3)$ upon the momentum eigenstate $|0\rangle_{p_2}$. In the Heisenberg picture this may be written as

$$q_2 = q_2^{(0)}, \quad p_2 = p_2^{(0)} + 3\gamma q_2^2, \quad (1)$$

where $p_2^{(0)}|0\rangle_{p_2} = 0$.

The two-mode entangling operation $C_Z \sim \exp(iq_1q_2)$ transforms the system variables as

$$\begin{aligned} q_1' &= q_1 & q_2' &= q_2 \\ p_1' &= p_1 + q_2, & p_2' &= p_2 + q_1. \end{aligned} \quad (2)$$

In order to illustrate the system evolution before the measurement, we represent initial state of both oscillators as a statistical ensemble of canonical coordinates and momenta $\{q_i, p_i\}$ in a semiclassical manner. Since the uncertainty region of the state $|0\rangle_{p_2}$ is horizontal straight line, by applying (1) one arrives to an approximate representation of the cubic phase state support in the form of a parabola.

In general, the cubic phase state Wigner function [16] has fringes and negative values in some areas on the phase plain, which of course is missing in the simplified picture. Nevertheless, in the following we demonstrate that this illustrative approach provides a hint allowing to infer the cat state emergence, and even to deduce its properties under certain limitations.

In Fig. 1 quadrature amplitudes are randomly chosen on the phase plane within the uncertainty region of the corresponding field and represented by the arrows. Next, the transformation (2) is applied.

In the Schrödinger picture, the initially prepared independent input field and ancilla states are

$$|\psi_1\rangle = \int dx_1 \psi(x_1)|x_1\rangle,$$

$$|\psi_2\rangle = e^{i\gamma q_2^3} \int dx_2 |x_2\rangle = \int dx_2 e^{i\gamma x_2^3} |x_2\rangle,$$

correspondingly, where the input field coordinate wave function is $\psi(x_1)$. The cubic phase state of the ancillary oscillator emerges during non-Gaussian evolution of the unnormalizable momentum eigenstate $|0\rangle_{p_2}$. The two-mode entangling operation $\exp(iq_1q_2)$ acts on the initial state with the outcome

$$|\psi_{12}\rangle = \int dx_1 dx_2 \psi(x_1) e^{ix_2(x_1 + \gamma x_2^2)} |x_1\rangle |x_2\rangle. \quad (3)$$

In order to describe measurement-induced state reduction, we represent the state (3) in the measurement basis, using standard definitions

$$|x\rangle = \frac{1}{\sqrt{2\pi}} \int dy e^{-ixy} |y\rangle, \quad |y\rangle = \frac{1}{\sqrt{2\pi}} \int dx e^{ixy} |x\rangle.$$

In the following, we use x and y to label the coordinate and momentum eigenstates correspondingly. The state (3) may be written as

$$\frac{1}{\sqrt{2\pi}} \int dy_2 |y_2\rangle \int dx_1 dx_2 \psi(x_1) e^{ix_2(x_1 - y_2 + \gamma x_2^2)} |x_1\rangle.$$

The ancilla momentum measurement with the outcome y_m projects the first oscillator into the state with the wave function $\tilde{\psi}(x) = \mathcal{N}\psi(x)\varphi_\gamma(x - y_m)$. Here \mathcal{N} is the normalization coefficient and the added factor is expressed in terms of the Airy function,

$$\varphi_\gamma(x - y_m) = \frac{1}{\sqrt{2\pi}} \int dx' e^{ix'(x - y_m + \gamma x'^2)} = \quad (4)$$

$$\left(\sqrt{2\pi}/(3\gamma)^{1/3}\right)\text{Ai}\left((x-y_m)/(3\gamma)^{1/3}\right).$$

The output field coordinate x in (4) is in the range that supports the spatial distribution $|\psi(x)|^2$. A Schrödinger cat state conditionally arise when the measured ancilla momentum is large enough, $y_m > x$ for all x within this range.

For such measurement outcome, the polynomial $x'(x - y_m + \gamma x^2)$ in the exponent can be approximated with quadratic expression. In Fig. 1 (upper right corner) this corresponds to the limit where the curve that approximately represents the displaced cubic phase state might be replaced with straight lines in a vicinity of two intersections with the horizontal line indicating the measured momentum.

The stationary phase points are $x'_s = \pm\sqrt{(\gamma_m - x)/3\gamma}$, and the exponent in (4) is represented near these points as

$$\mp \frac{2}{3\sqrt{3\gamma}}(y_m - x)^{3/2} \pm \sqrt{3\gamma(y_m - x)} \left(x' \mp \sqrt{(y_m - x)/3\gamma}\right)^2.$$

The factor (4) becomes a sum of two independent integrals. By making use of

$$\int dx e^{i\kappa x^2} = \exp\left(i\frac{\pi}{4}\right) \sqrt{\frac{\pi}{\kappa}},$$

we finally identify the output field state wave function as a superposition of two distinguishable components,

$$\tilde{\psi}(x) = \mathcal{N}\psi(x) \left(\varphi_\gamma^{(+)}(x - y_m) + c. c.\right), \quad (5)$$

where

$$\varphi_\gamma^{(+)}(x - y_m) = \quad (6)$$

$$\exp\left[i\left(\frac{\pi}{4} - \frac{2}{3\sqrt{3\gamma}}(y_m - x)^{3/2}\right)\right] (12\gamma(y_m - x))^{-1/4}.$$

For $y_m \gg |x|$ within the relevant range, the exponent can be linearized in x/γ_m . This yields $\varphi_\gamma^{(+)}(x - y_m) \sim \exp(i\sqrt{y_m/3\gamma}x)$, which means that this gate conditionally projects the initial state into the superposition of two “copies” with well-defined opposite shift in momentum of $\pm\sqrt{y_m/3\gamma}$, in agreement with Fig. 1 (upper left corner). If this measurement-dependent shift is larger than the range of momentum spanned by the input state, the gate output state is nothing but a Schrödinger cat.

The factor added by the gate is represented [30] in Fig. 2. As seen from the figure, the exact factor $\varphi_\gamma(x - y_m)$ and the approximate one are in perfect agreement except for a small range of coordinate. For $x \approx y_m$, the approximate solution diverges since the approximation of two distinguishable crossings does not work near the bottom of parabola in Fig. 1. In this area the non-classical properties of the cubic phase state Wigner function are most pronounced. The exact result exhibits fast decrease

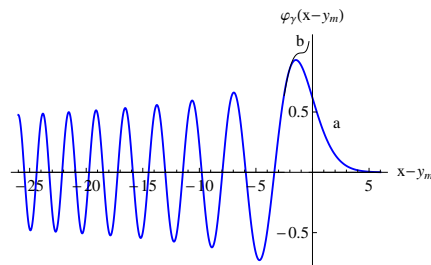


FIG. 2: The factor $\varphi_\gamma(x - y_m)$ added by the gate to the initial coordinate wave function by the outcome y_m of ancilla momentum measurement. Here $\gamma = 1$, curve a was evaluated numerically from the representation of the Airy function through the integral (4), curve b corresponds to the approximate solution (5,6).

in the region $y_m < x$ which is unreachable for the measurement in classical picture.

The cat-breeding transformations of an arbitrary input state may be combined with standard Gaussian operations such as displacement, rotation, squeezing and shearing. By establishing the measurement window with a needed precision (which of course has effect on the success probability), one can conditionally generate on demand complex cat-like structures on the phase plane.

There is a variety of measurement-based CV Gaussian schemes of quantum information, such as quantum teleportation and dense coding, quantum repeaters, cluster model of quantum computing, etc. The Gaussian schemes with measurement and feedforward can be effectively described both in the Schrödinger and the Heisenberg picture, where the last one offers a possibility to include noise sources and imperfections in the scheme [5–9, 29] and provides in many cases an intuitively clear illustration of the processes in the device.

Various approaches towards more general configurations seeded with non-Gaussian gates were developed, and some works analyzed such gates both in the Schrödinger and the Heisenberg picture [20, 21].

The non-Gaussian gate described here exploits the same key elements (that is, a nonlinear phase state, an entangling Gaussian gate and homodyne measurement) as many other schemes. This gate provides an instructive example where the Heisenberg picture, when applied within the same paradigm as in the measurement based Gaussian quantum information, fails due to the presence of non-Gaussianity.

The transformations (1, 2) which describe the system unitary evolution in the Heisenberg picture before the measurement may be combined as

$$\begin{aligned} q'_1 &= q_1 & q'_2 &= q_2 \\ p'_1 &= p_1 + q_2, & p'_2 &= p_2 + q_1 = p_2^{(0)} + 3\gamma q_2^2 + q_1. \end{aligned}$$

Following standard for Gaussian networks approach, we describe the ancilla momentum measurement by substi-

tuting the measurement outcome y_m for the operator-valued amplitude p'_2 . This yields $3\gamma q_2^2 = y_m - q_1 - p_2^{(0)}$. Then q_2 is excluded from p'_1 , and we arrive at the target oscillator output quadrature amplitudes

$$\begin{aligned} q_1^{(out)} &= q_1 \\ p_1^{(out)} &= p_1 \pm (3\gamma)^{-1/2} \sqrt{y_m - q_1 - p_2^{(0)}}. \end{aligned} \quad (7)$$

Since statistical averaging of the canonical variables and their momenta in the Heisenberg picture must be performed with the system initial state and in view of $p_2^{(0)}|0\rangle_{p_2} = 0$, we drop $p_2^{(0)}$ here.

There are evident problems with this result which make it useless for the standard task: to evaluate correlation functions and momenta of the output physical quantities. First, the expression for $p_1^{(out)}$ is nonunique. Secondly, as far as the factor $\varphi_\gamma(x - y_m)$ is not equal zero beyond the classically unreachable region, the measurement outcomes $y_m < x$ are possible which makes $p_1^{(out)}$ look non-Hermitian.

On the other hand, a comparison with the results derived above from the Schrödinger picture makes it clear that just this nonuniqueness manifests emergence of a Schrödinger cat state.

It is worth noting that even when the output physical quantities emerge as single valued, this does not guarantee correct description of a CV non-Gaussian scheme with

measurement and feedforward, if the Heisenberg picture is used within the same paradigm as in Gaussian quantum information, as we shall discuss elsewhere.

In conclusion, we have presented non-Gaussian CV gate which is able to conditionally produce a superposition of two “copies” of an arbitrary input state, well separated in the coordinate and momentum plane, which corresponds to the emergence of Schrödinger cat state. In analogy to some other proposals, the scheme exploits the same key elements, that is, ancillary cubic phase state and C_Z Gaussian gate, but applies homodyne measurement which provides a nonunique information about the target system physical quantities. One can infer from this result that a CV quantum network with embedded non-Gaussian gates of general kind may experience measurement-induced evolution into a Schrödinger cat state of an arbitrary complexity.

The scheme presented here also provides an instructive example of problems which may arise by the extension of the Heisenberg picture, as it is commonly used in various CV Gaussian schemes of quantum information, onto the measurement-induced evolution of CV non-Gaussian networks.

I thank Nikolay N. Bezuglov for fruitful discussions. This research was supported by the Russian Foundation for Basic Research (RFBR) under the projects 18-02-00648-a and 19-02-00204-a.

-
- [1] S. Lloyd and S. L. Braunstein, Phys. Rev. Lett. **82**, 1784 (1999).
- [2] S. L. Braunstein and P. van Loock, Rev. Mod. Phys. **77**, 513 (2005).
- [3] A. Furusawa, J. L. Sørensen, S. L. Braunstein, C. A. Fuchs, H. J. Kimble, and E. S. Polzik, Science **282**, 706 (1998).
- [4] X. Li, Q. Pan, J. Jing, J. Zhang, C. Xie, and K. Peng, Phys. Rev. Lett. **88**, 047904 (2002).
- [5] M. Gu, C. Weedbrook, N. C. Menicucci, T. C. Ralph, and P. van Loock, Phys. Rev. A **79**, 062318 (2009).
- [6] C. Weedbrook, S. Pirandola, R. Garcia-Patron, N. J. Cerf, T. C. Ralph, J. H. Shapiro, and S. Lloyd, Rev. Mod. Phys. **84**, 621 (2012).
- [7] R. Ukai, *Multi-Step Multi-Input One-Way Quantum Information Processing with Spatial and Temporal Modes of Light* (Springer, Tokyo, Japan, 2015).
- [8] S. Yokoyama, R. Ukai, S. C. Armstrong, C. Sornphiphatphong, T. Kaji, S. Suzuki, J. Yoshikawa, H. Yonezawa, N. C. Menicucci, and A. Furusawa, Nat. Photonics **7**, 982 (2013).
- [9] J. Roslund, R. Medeiros de Araújo, S. Jiang, C. Fabre, and N. Treps, Nat. Photon. **8**, 109 (2014).
- [10] S. D. Bartlett, B. C. Sanders, S. L. Braunstein, and K. Nemoto, Phys. Rev. Lett. **88**, 097904 (2002).
- [11] U. L. Andersen, J. S. Neergaard-Nielsen, P. van Loock, and A. Furusawa, Nat. Phys. **11**(9), 713 (2015).
- [12] Y.-S. Ra, A. Dufour, M. Walschaers, C. Jacquard, T. Michel, C. Fabre, and N. Treps, Nat. Phys. **16**, 144 (2020).
- [13] D. Gottesman, A. Kitaev, and J. Preskill, Phys. Rev. A **64**, 012310 (2001).
- [14] S. D. Bartlett and B. C. Sanders, Phys. Rev. A **65**, 042304 (2002).
- [15] S. Sefi and P. van Loock, Phys. Rev. Lett. **107**, 170501 (2011).
- [16] S. Ghose and B. C. Sanders, J. Mod. Opt. **54**, 855 (2007).
- [17] P. Marek, R. Filip, and A. Furusawa, Phys. Rev. A **84**, 053802 (2011).
- [18] M. Yukawa, K. Miyata, H. Yonezawa, P. Marek, R. Filip, and A. Furusawa, Phys. Rev. A **88**, 053816 (2013).
- [19] K. Marshall, R. Pooser, G. Siopsis, and C. Weedbrook, Phys. Rev. A **91**, 032321 (2015).
- [20] K. Miyata, H. Ogawa, P. Marek, R. Filip, H. Yonezawa, J.-I. Yoshikawa, and A. Furusawa, Phys. Rev. A **93**, 022301 (2016).
- [21] P. Marek, R. Filip, H. Ogawa, A. Sakaguchi, S. Takeda, J.-I. Yoshikawa, and A. Furusawa, Phys. Rev. A **97**, 022329 (2018).
- [22] D. W. Moore, Phys. Rev. A **100**, 062301 (2019).
- [23] E. Schrödinger, Naturwissenschaften **23**(48), 807 (1935).
- [24] M. Mirrahimi, Z. Leghtas, V. V. Albert, S. Touzard, R. J. Schoelkopf, L. Jiang, and M. H. Devoret, New J. Phys. **16**, 045014 (2014).
- [25] B. Yurke and D. Stoler, Phys. Rev. Lett. **57**, 13 (1986).
- [26] A. Ourjoumtsev, H. Jeong, R. Tualle-Brouri, and P. Grangier, Nature **448**, 784 (2007).
- [27] J. Etesse, R. Blandino, B. Kanseri, and R. Tualle-Brouri,

- New J. Phys. **16**, 053001 (2014).
- [28] J. Etesse, M. Bouillard, B. Kanseri, and R. Tualle-Brouri, Phys. Rev. Lett. **114**, 193602 (2015).
- [29] S. B. Korolev, T. Yu. Golubeva, and Yu. M. Golubev, Laser Phys. Lett. **17**, 035207 (2020).
- [30] In order to ensure better convergency of the improper integral (4) that represents the Airy function, one can apply deformation of the integration contour in the complex plain by assuming $x' = ze^{i\pi/6}$ for $z > 0$.